

# Preclinical Antitumor Activity of BMS-214662, a Highly Apoptotic and Novel Farnesyltransferase Inhibitor

William C. Rose, Francis Y. F. Lee, Craig R. Fairchild, Mark Lynch, Thomas Monticello, Robert A. Kramer, and Veeraswamy Manne<sup>1</sup>

Pharmaceutical Research Institute, Oncology Drug Discovery, Bristol-Myers Squibb Company, Inc., Princeton, New Jersey 08543

## ABSTRACT

**BMS-214662 is a potent and selective inhibitor of farnesyltransferase (FTI). In rodent fibroblasts transformed by oncogenes, BMS-214662 reversed the H-Ras-transformed phenotype but not that of K-Ras or other oncogenes. In soft agar growth assays, BMS-214662 showed good potency in inhibiting H-ras-transformed rodent cells, A2780 human ovarian carcinoma tumor cells, and HCT-116 human colon carcinoma tumor cells. Inhibition of H-Ras processing in HCT-116 human colon tumor cells was more rapid than in H-Ras-transformed rodent fibroblast tumors. BMS-214662 is the most potent apoptotic FTI known and demonstrated broad spectrum yet robust cell-selective cytotoxic activity against a panel of cell lines with diverse histology. The presence of a mutant *ras* oncogene was not a prerequisite for sensitivity. Athymic and conventional mice were implanted s.c. with different histological types of human and murine tumors, respectively. BMS-214662 was administered both parenterally and p.o. and was active by all these routes. Curative responses were observed in mice bearing staged human tumor xenografts including HCT-116 and HT-29 colon, MiaPaCa pancreatic, Calu-1 lung, and EJ-1 bladder carcinomas. A subline of HCT-116, HCT-116/VM46, resistant to many standard cytotoxic agents by means of a multiple drug resistance mechanism, remained quite susceptible to BMS-214662, and borderline activity was achieved against N-87 human gastric carcinoma. Two murine tumors, Lewis lung carcinoma and M5076 sarcoma, were insensitive to the FTI. In a study performed using Calu-1 tumor-bearing mice, no obvious schedule dependency of BMS-214662 was observed. The FTI, BMS-214662, demonstrated broad spectrum activity against human tumors, but murine tumors were not as sensitive.**

## INTRODUCTION

The proteins encoded by the *ras* genes are guanine nucleotide binding proteins that associate with the inner plasma membrane and transduce external signals to the interior of the cell. Functionally, Ras proteins oscillate between active Ras.GTP and inactive Ras.GDP states (1, 2) in a highly regulated manner. Activation of p21 Ras, as represented by increased levels of the p21 Ras.GTP complex, occurs in response to a large variety of extracellular stimuli including growth signals (3). The signal is normally dissipated quickly by hydrolysis of Ras-bound GTP to GDP (4, 5). Mutated Ras proteins are locked in the persistently activated Ras.GTP state (6, 7) and cause malignant transformation. Activating mutations in the *ras* genes are among the more common genetic aberrations known in human cancers (1, 8), particularly in pancreatic (85%) and colon carcinomas (40%). Mutated Ras oncoproteins contribute significantly to the malignant properties of the cancer cells.

Although it would be desirable to develop therapeutic agents that specifically target oncogenic Ras activity, such compounds have not been identified despite concerted efforts over the past decade. The search for inhibitors of Ras function has intensified in the past 11

years after the discovery that Ras proteins are among the limited set of known proteins that undergo farnesylation. Farnesylation of Ras proteins is required for their membrane association, which in turn is critical for their biological functions. When farnesylation is blocked, the function of Ras proteins is severely impaired because of the inability of the nonfarnesylated protein to anchor to the membrane (9–11). Therefore, FT,<sup>2</sup> the enzyme that catalyzes the farnesylation reaction, has become an important target for the design of novel anticancer agents (12–18).

Although early studies indicated that FTIs do selectively affect the growth of Ras-transformed cells and exhibit antitumor activity in preclinical animal models (19–25), evolving recent studies portray a highly complex nature to the biology and preclinical antitumor activity of FTIs (26–36). In FTI-treated cells, K-Ras and N-Ras proteins have been shown to undergo geranylgeranylation (37, 38) catalyzed by GGTI and potentially remain functional. However, FTIs, in general, demonstrate *in vitro* and *in vivo* activity against tumor cells bearing K-Ras mutations (23, 39–41). Moreover, no clear correlation between Ras mutation status and FTI sensitivity has been observed by several investigators (23, 39–41). Whereas some investigators effort championed RhoB and centromere-associated CENP-E and CENP-F as the molecular targets of FTIs in all or some tumor cells, there remains no consensus as to the relevant target(s) of FTIs that can explain the mosaic pharmacology of FTIs (42–48).

BMS-214662, an imidazole-containing tetrahydrobenzodiazepine, is a non-thiol, non-peptide small molecule inhibitor (49). The present report describes the pharmacology of BMS-214662 and its broad spectrum antitumor activity against a variety of human tumor xenografts. Its broad spectrum antitumor activity, by both parenteral and oral routes of administration, was found to be of sufficient magnitude to provide the basis of further development toward clinical trials.

## MATERIALS AND METHODS

**Drug Preparation.** For *in vitro* studies, the hydrochloride salt of BMS-214662 was dissolved in DMSO with dilutions made using either water or RPMI 1640 (Life Technologies, Inc.) plus 10% fetal bovine serum (Life Technologies, Inc.). The compound was dissolved in ethanol, followed by dilution with water to a final ethanol concentration of 10% for many *in vivo* studies. This latter vehicle was used for all i.p. and oral (p.o.) administrations. A formulation of 5% Tween 80 in water (pH 2.9–3.4) was used for i.v. administrations.

**Farnesyltransferase.** A pAcUW31-based baculovirus transfer vector, pML88, encoding both the  $\alpha$  and  $\beta$  subunits of hFT, was constructed. After cotransfection of pML88 and wild-type baculovirus DNA into insect cells, recombinant baculoviruses were isolated, purified, and analyzed for their ability to overexpress biologically active hFT. High levels of hFT were

Received 5/2/01; accepted 8/15/01.

The costs of publication of this article were defrayed in part by the payment of page charges. This article must therefore be hereby marked *advertisement* in accordance with 18 U.S.C. Section 1734 solely to indicate this fact.

<sup>1</sup> To whom requests for reprints should be addressed, at Oncology Drug Discovery, Department of Signal Transduction and Gene Expression, K22-07, Bristol-Myers Squibb Co., P. O. Box 4000, Princeton, NJ 08543. Phone: (609) 252-5832; Fax: (609) 252-6051; E-mail: Veeraswamy.manne@bms.com.

<sup>2</sup> The abbreviations used are: FT, farnesyltransferase; hFT, human FT; FTI, farnesyltransferase inhibitor; GGTI, geranylgeranyl transferase inhibitor; MDR, multidrug resistant; BMS, Bristol-Myers Squibb Company; ABAE, adult bovine aortic endothelial; LL, Lewis lung; TUNEL, terminal deoxynucleotidyl transferase-mediated dUTP nick end labeling; LCK, log cell kill; IC<sub>50</sub>, compound concentration needed to inhibit cell growth by 50% relative to untreated control cell growth; MEK, mitogen-activated protein kinase; MTD, maximum tolerated dose; MTS, [3-(4,5-dimethylthiazol-2-yl)-5-(3-carboxymethoxyphenyl)-2-(4-sulfenyl)-2H-tetrazolium, inner salt]; qd, every day; AI, apoptotic index; SAG, soft agar growth.

produced in cells infected with pML88 recombinant baculovirus for 48 h. A majority of the hFT was recovered in the soluble fraction and was purified to  $\geq 95\%$  purity by DE-52 and Phenyl Superose chromatography steps.

**GGTI.** A baculovirus expression construct containing the  $\alpha$  subunit of hFT was coinfecting into High Five insect cells with a baculovirus expression construct coding for the  $\beta$  subunit of human GGTI. After sonication, hGGTI was purified from the insect cell supernatant by DE-52 and Phenyl Superose chromatography steps. The purified enzyme was estimated to be at least 80% pure.

**Cell Lines and Culture.** KNIH, Rat1CVLS, Ras-GG, myr-Ras, and K-Ras4B cells have been described previously (25). RC-165 cells are Rat1 cells transformed by human genomic K-Ras4B DNA (contains the human K-ras4B minigene with a G418 selectable marker with cys12 mutation). v-Raf cells are NIH 3T3 cells transformed by a recombinant clone carrying gag v-Raf and neoR in an MSV vector (50). c-Raf cells are NIH 3T3 cells transformed by activated c-Raf (22W mutant) and were described earlier (51). MEK2 cells are Rat1 cells transformed by human MEK-1 cDNA with two activating mutations, one at codon 218 (serine to aspartate) and the other at codon 222 (serine to aspartate). The cell line panel was composed of: human ovarian carcinomas (A2780/DDP-S, A2780/DDP-R, A2780/TAX-S, A2780/TAX-R, and OVCAR-3); human breast carcinomas (MCF-7 and SKBR-3); human prostate carcinomas (LNCAP and PC-3); human colon carcinomas (HCT-116, HCT-116/VM46, HCT-116/VP35, Caco-2, LS 174T, and MIP); human lung carcinomas (A549 and LX-1); a human squamous cell carcinoma (A431); human leukemias (CCRF-CEM, HL-60, and K562); ABAE cell line; a mouse lung carcinoma (M109); and a p53<sup>-/-</sup> mouse lung fibroblast cell line, MLF, isolated from p53 knock-out mice. The HCT-116/VM46 cell line is a MDR variant of the parental HCT-116 cells and overexpresses P-glycoprotein (52). The HCT-116/VP35 cell line is a variant that has low topoisomerase II levels and is resistant to etoposide (52). The A2780/DDP-R cell line is resistant to cisplatin relative to the parental A2780/DDP-S cells. A tubulin mutation is present in the A2780/TAX-R cells, which are resistant to paclitaxel relative to the parental A2780/TAX-S cells (both provided by Dr. Tito Fojo, National Cancer Institute, Bethesda, MD; Ref. 53).

Rat1CVLS, RC-165, K-Ras4B, Myristoyl-Ras, and GG-Ras cells were grown in DMEM with 110 mg/l sodium pyruvate supplemented with 10% FBS (Colorado Serum Co.; not heat inactivated) in a 95% humidified CO<sub>2</sub> (6–7%) incubator maintained at 37°C. All other rodent cells were grown in DMEM high glucose supplemented with 5% calf serum (Colorado Serum Co.). Mammalian cells were maintained in logarithmic growth in RPMI 1640 (Life Technologies, Inc.), 5 mM HEPES buffer, and 10% fetal bovine serum (Life Technologies, Inc.) and were passed once per week. ABAE cells (a primary cell line) were grown in RPMI 1640 containing 2.0 ng/ml of basic fibroblast growth factor.

**Mice.** BALB/c background athymic (nude) female mice and C57BL/6 and (C57BL/6  $\times$  DBA/2)F<sub>1</sub> conventional mice, all  $\sim 5$  weeks of age, were purchased from Harlan Sprague Dawley (Indianapolis, IN). They were provided with food and water *ad libitum*. All studies involving these animals were conducted in accordance with NIH and our BMS animal care and use guidelines.

**Tumors.** The following human tumor lines were used: HCT-116 colon, HCT-116/VM46 colon, Calu-1 lung, EJ-1 bladder, MiaPaCa-2 pancreatic, N-87 gastric, and HT-29 colon carcinomas. Two murine tumor models, LL carcinoma and M5076 sarcoma, were also used. The human tumors were passaged *s.c. in vivo* at approximately 2–3-week intervals. The murine tumors were passaged *s.c.* in C57BL/6 mice at 2-week intervals. The following Ras mutations are known to exist and were confirmed at BMS in these tumors: HCT-116 and the HCT-116/VM46 subline (K-Ras); Calu-1 (K-Ras); EJ-1 (H-Ras); MiaPaCa-2 (K-Ras); HT-29 (none); LL (none); and M5076 (none).

**Pharmacology Assays.** The assays for prenyltransferase, reversion, SAG, and H-Ras processing inhibition were carried out as described earlier (18, 25). Apoptosis was measured using the cell death detection ELISAplus kit (nucleosomal DNA ELISA assay) supplied by Boehringer Mannheim and Apo-direct flow cytometry kit (TUNEL assay) supplied by Pharmingen. The instructions supplied by the kit manufacturer were followed.

**In Vitro Cytotoxicity Assay.** *In vitro* cytotoxicity was assessed by a vital dye assay using a tetrazolium salt, MTS. Cells were seeded in 96-well microtiter plates, and 24 h later, BMS-214662 was added at various concentrations. The cells were incubated at 37°C for 72 h, at which time MTS in combination

with phenazine methosulfate was added. After an additional 3 h, the absorbance was measured at 492 nm, and the growth inhibition results were eventually expressed as IC<sub>50</sub>s.

The IC<sub>50</sub>s for BMS-214662 were calculated and expressed graphically as a mean bar graph on a log scale for each cell line exposed to the compound. A geometric mean of the log IC<sub>50</sub>s was also determined. The difference between the mean log IC<sub>50</sub> and each individual cell line's log IC<sub>50</sub> was calculated and plotted in a mean bar graph. Bars that project to the right represent cells that are more sensitive than the mean IC<sub>50</sub> for all of the cell lines. Bars that project to the left represent cell lines that are less sensitive (more resistant) than the mean.

**Efficacy Testing.** Briefly, (C57BL/6  $\times$  DBA/2)F<sub>1</sub> mice were implanted *s.c.* with tumor fragments (M5076 and LL), and treatments began 1 day after tumor implant. Treatments were administered either *i.v.* or *i.p.* The specific treatments evaluated are described in "Results." For human tumor xenograft tests, nude mice were implanted *s.c.*, and treatments (*p.o.*, *i.v.*, or *i.p.*) were begun when sufficient mice bearing tumors of a predetermined size were distributed into various control and treatment groups. The "predetermined size" initially was typically  $\sim 100$  mg, but the stringency of test conditions eventually increased, and many experiments (specifically described) involved the use of larger, 200–400 mg tumors. Treatments involving various schedules were used, and they are described in "Results."

Assessment of antitumor effectiveness was made by determining the relative median times for control (C) and treated (T) mice to grow tumors to a target size. The target size was 1 g for M5076 and LL and 400–500 mg for all of the human tumor models. The delay in tumor growth ( $T - C$ , days) was converted to gross LCK values by taking into account the tumor volume doubling times of control groups in each individual experiment. A LCK of 1 or better was considered an active result. Cures were also used to assess activity. A mouse was considered cured when no mass  $< 35$  mg was present at the site of tumor implant after a number of days after treatment had elapsed equivalent to  $> 10$  tumor volume doubling times in that experiment. Therapeutic results were reported at the optimal dose, and results were not used if more than one death occurred in the treated group. A MTD, although often synonymous with the optimal dose, is defined as a dose immediately below that causing unacceptable toxicity (*i.e.*, more than one death), or in the absence of any deaths, was assumed when accompanied by  $> 20\%$  body weight loss. There were typically seven to eight mice per treatment and control groups.

***i.v.* Infusion of Mice.** Infusional *i.v.* drug delivery via the tail vein was accomplished using the L-CATH Neonatal Catheter System (Luther Medical Products, Inc., Tustin, CA). The 28-gauge (0.4-mm outside diameter) catheter was inserted in the tail vein  $\sim 5$  cm from the base and advanced 4 cm into the vein. The catheter was stabilized with Nexaband Liquid (Henry Schein, Inc.) and then firmly secured with Tegaderm (Henry Schein, Inc.). The entire tail and catheter were then inserted into a protective sheath, and then the mice were tied to a swivel. Mice were moving freely during the entire infusion period.

***In Vivo-in Vitro* Tumor Excision Clonogenic Cell Survival Assay.** After 24-h drug infusions of varying doses, tumors were excised from mice, minced with scissors, and dissociated using an enzyme mixture consisting of 0.025% collagenase (Sigma Chemical Co., St. Louis, MO), 0.05% Pronase (Calbiochem, La Jolla, CA), and 0.04% DNase (Sigma Chemical Co.) for 1 h at 37°C. After removal of debris, by passing the tumor suspensions through 70- $\mu$ m nylon screens, the cells were washed in PBS, counted, and plated at specified numbers for determination of colony formation capacity.

**Apoptosis in Tumors.** Mice ( $n =$  two to three/group) implanted with HCT-116 xenografts were administered a single dose of BMS-214662 at 250 mg/kg *i.v.*, 300 mg/kg *i.p.*, or 400 mg/kg *p.o.* An additional group ( $n = 2$ ) received 400 mg/kg BMS-214662 daily for 2 days (administered *p.o.* on day 1 and *i.p.* on day 2). Nontreated mice ( $n = 4$ ) with time-matched HCT-116 tumors served as controls. Tumors were collected at 24 h after dose, processed following standard methods, sectioned, and stained with H&E. Serial sections of each tumor were processed for *in situ* apoptotic cell labeling by the TUNEL method (ApoTag; Oncor).

AIs of the tumor, defined as the percentage of apoptotic tumor, was reported previously (54). Apoptotic tumor cells were identified by light microscopy based on positive TUNEL staining and/or defined morphological criteria (55). For each tumor, 10–30 random fields, which excluded necrotic areas, were evaluated at  $\times 200$ , and the total number of tumor cells and apoptotic cells were enumerated per field. AIs were calculated by dividing the total number of

apoptotic tumor cells by the total cell population  $\times 100$ . Mean AIs were calculated for each group.

## RESULTS

### In Vitro Activity

BMS-214662 is a lead compound in the tetrahydrobenzodiazepine class of FTIs discovered at BMS and is presently being evaluated in Phase I clinical trials (Fig. 1). BMS-214662 is a potent inhibitor of human FT as assayed *in vitro* using H-Ras or K-Ras as the farnesyl acceptor substrates. The FT inhibitory potency *versus* H-Ras and K-Ras were determined in several independent experiments, and the results are summarized in Table 1. The mean  $IC_{50}$  and  $IC_{90}$  (50 and 90% inhibitory concentrations) for H-Ras farnesylation were determined to be 1.3 and 18 nM, respectively. BMS-214662 inhibited H-Ras farnesylation more potently than K-Ras farnesylation ( $IC_{50}$ , 1.3 nM for H-Ras *versus* 8.4 nM for K-Ras).

The ability of BMS-214662 to inhibit GGTI was determined in an *in vitro* assay using purified recombinant hGGTI. BMS-214662 is a poor inhibitor of GGTI as assayed *in vitro* using H-RasCVLL and K-Ras proteins as the geranylgeranyl acceptor substrates. The  $IC_{50}$ s for geranylgeranylation of Ras-CVLL and K-Ras protein substrates are 1300 and 2300 nM, respectively (Table 1). Thus, BMS-214662 is  $>1000$ -fold selective for hFT over human hGGTI.

### Activity Spectrum of BMS-214662 in Cells

**Reversion and SAG.** Two cell-based assays, the reversion assay and the SAG assay, were used primarily for evaluating the cell activity of BMS-214662. Both assays measure the response of cells because oncogenic Ras function is impaired due to FT inhibition. BMS-214662 reverts H-Ras-transformed Rat1 cells to a normal flat monolayer phenotype in cell cultures at low micromolar concentrations. Near complete reversion occurred when cells were exposed for 72 h at 0.3  $\mu$ M BMS-214662 (Table 2). The transformed properties of H-Ras proteins that have been engineered to function independently of farnesylation such as N-myristoyl Ras (MyrRas) or geranylgeranyl Ras (RasGG) are not affected by BMS-214662 (no reversion at 2.5  $\mu$ M), suggesting Ras farnesylation as the specific target. In addition, the transformed properties of v-Raf or MEK, which function downstream of Ras, are also not affected, thus confirming the specificity of BMS-214662 (Table 2). BMS-214662 failed to revert the K-Ras-transformed cells (KNIH, RC-165, and K-Ras4B val12) phenotype.

BMS-214662 inhibited the SAG of H-Ras-transformed cells, K-Ras-transformed cells, and several human tumor cells such as HCT-116, MiaPaCa-2, and A2780. BMS-214662 is particularly potent against H-Ras-transformed rodent cells, A2780 human ovarian carcinoma cells, and HCT-116 human colon tumor cells. Near complete inhibition of the SAG of these sensitive cells occurred at 0.15  $\mu$ M (Table 2). K-Ras-transformed rodent cells, MIP human colon tumor

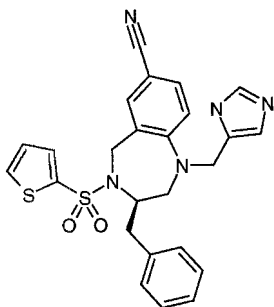


Fig. 1. Structure of BMS-214662.

Table 1 Mean  $IC_{50}$  and  $IC_{90}$  concentrations of BMS-214662 for FT and GGTI

Enzyme	Protein substrate	Prenyl donor	n	Mean $IC_{50}$ (nM)	Mean $IC_{90}$ (nM)
FT	H-Ras	FPP	52	1.3	18
FT	K-Ras	FPP	7	8.4	108
GGTI	K-Ras	GGPP	2	1900	17700
GGTI	H-RasCVLL	GGPP	2	1400	5600

Table 2 Cell activity of BMS-214662

Cell type (mutation)	Assay used	$IC_{50}$ ( $\mu$ M)	$IC_{90}$ ( $\mu$ M)
Rat1-CVLS (H-Ras)	Reversion assay	0.1	0.31
RC-165 (K-Ras)	Reversion assay	$>2.5$	$>2.5$
KNIH (K-Ras)	Reversion assay	$>2.5$	$>2.5$
K-Ras4B (K-Ras)	Reversion assay	$>2.5$	$>2.5$
MEK2	Reversion assay	$>2.5$	$>2.5$
C-Raf	Reversion assay	$>2.5$	$>2.5$
v-Raf	Reversion assay	$>2.5$	$>2.5$
Myristoyl-Ras	Reversion assay	$>2.5$	$>2.5$
GG-Ras	Reversion assay	$>2.5$	$>2.5$
44911 (H-Ras)	SAG assay	0.025	0.15
RC-165 (K-Ras)	SAG assay	0.3	0.62
MEK2	SAG assay	2.5	$>2.5$
HCT-116 (K-Ras)	SAG assay	0.06	0.15
MIP (K-Ras)	SAG assay	0.3	0.6
A2780 DDP (wt)	SAG assay	0.08	0.15
A2780 tax22 (wt)	SAG assay	0.08	0.15
PC-3 (wt)	SAG assay	0.15	0.31
A2780s (wt)	SAG assay	0.04	0.08
MiaPaca-2 (K-Ras)	SAG assay	0.12	0.62

cells, and MiaPaCa-2 human pancreatic tumor cells require 0.6  $\mu$ M for complete inhibition. MEK-2-transformed cells are not dependent on Ras function for SAG and are not affected by BMS-214662 at concentrations up to 2.5  $\mu$ M.

**Inhibition of H-Ras Processing in H-Ras-transformed Rodent Cells.** To demonstrate that BMS-214662 inhibits Ras processing in cells and causes cytoplasmic localization of unmodified Ras proteins, we used H-Ras-transformed Rat1 CVLS cells. Cells were treated for 48 or 72 h with 0.1 or 0.5  $\mu$ M BMS-214662. Total cellular extracts were prepared and fractionated into soluble (S100) and particulate (P100) fractions. The Ras proteins in S100 and P100 fractions were immunoprecipitated with agarose-linked Y13-259 anti-Ras antibody, analyzed by SDS-PAGE, transferred to Immobilon-P membrane, and probed with H-Ras-specific antibody 146-03E4. The results, shown in Fig. 2A, indicate that a majority of Ras proteins were present in the particulate fraction in the untreated cells. After treatment with BMS-214662, Ras proteins localized to the soluble fraction, and this process occurred in a dose-dependent manner. Concentrations as low as 100 nM caused partial inhibition of Ras processing (as reflected in the shift to soluble fraction) in 48 h. Near complete depletion of H-Ras from the membrane fraction occurred at 500 nM. On the basis of results from several experiments, we conclude that complete inhibition of H-Ras processing in Rat1 CVLS cells requires 48–72 h of drug treatment.

**Inhibition of H-Ras Processing in HCT-116 Human Colon Tumor Cells.** Inhibition of H-Ras processing and accumulation of unmodified H-Ras proteins occurred much more readily in HCT-116 human colon tumor cells (Fig. 2B). In contrast to kinetics in Rat1 CVLS fibroblasts, the kinetics of disappearance of membrane-bound Ras were nearly complete in 24 h with as little as 100 nM BMS-214662. These results suggest that the turnover of membrane-bound farnesylated Ras may vary in different cell types and are consistent with various (6 and 20 h) half-lives reported for Ras proteins (56, 57).

**Lack of Inhibition of K-Ras Processing in HCT-116 Human Colon Tumor Cells.** Previous studies by others (37, 38, 58) showed that K-Ras and N-Ras proteins in rodent fibroblasts or human tumor cells are resistant to treatment with potent FT inhibitors. The K-Ras

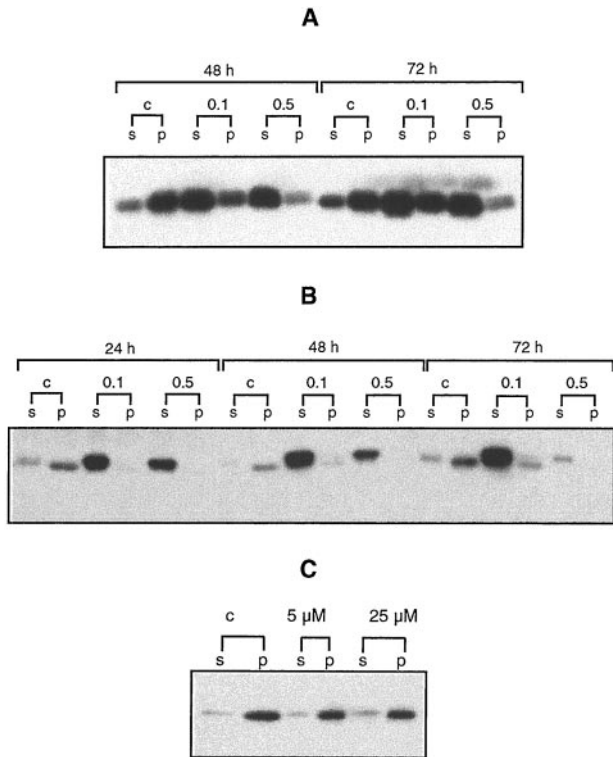


Fig. 2. A, H-Ras protein localization in H-Ras transformed Rat1 CVLS cells. B, H-Ras protein localization in HCT-116 human colon tumor cells. C, K-Ras protein localization in HCT-116 human colon tumor cells. Cells were exposed to BMS-214662 as indicated (c, control; 0.1, 0.1  $\mu\text{M}$ ; 0.5, 0.5  $\mu\text{M}$ ), and cell extracts were fractionated and processed as described in "Materials and Methods" for identifying H-Ras proteins. s, soluble fraction; p, particulate fraction.

and N-Ras proteins remained associated with membranes, although H-Ras proteins were localized to the cytosolic fraction during FTI treatment. Similarly, BMS-214662 failed to cause cytoplasmic localization of K-Ras proteins in HCT-116 cells. Treatment of cells with concentrations as high as 25  $\mu\text{M}$  for 24 h did not alter the amount of K-Ras proteins in the membranes, and there was no apparent increase in the amount of soluble (cytosolic) K-Ras proteins (Fig. 2C). These results are consistent with BMS-214662 being highly specific for FT over GGTI and the apparent ability of GGTI to geranylgeranilate K-Ras proteins when FT is inhibited in cells (37, 38, 58).

**Cytotoxicity of BMS-214662.** The FT inhibitory potencies and cell activities of tetrahydrobenzodiazepine FTIs and many other classes of FTIs are comparable (20, 23–25, 40, 41, 49). In many cell types, low  $\mu\text{M}$  concentrations of these inhibitors block Ras farnesylation to near completion. Although many of these other classes, in particular tetrapeptide-based inhibitors, are known to be nontoxic at high  $\mu\text{M}$  concentrations, the tetrahydrobenzodiazepine inhibitors including BMS-214662, are toxic to cells at 2–10  $\mu\text{M}$  concentrations. Cytotoxicity seems to be unrelated to complete inhibition of Ras processing and signaling, because BMS-214662 displayed toxicity to H-Ras, H-RasCVLL, and MyrH-Ras transformed Rat1 cells at similar concentrations. In the latter cells, Ras functions independently of farnesylation, and therefore FTIs should be nontoxic if toxicity is attributable predominantly to Ras inhibition *per se*. Similar observations were made with c-Raf, v-Raf, and MEK-2 transformed cells, which are Ras independent. Although these results do not eliminate the possibility that FT inhibition and/or processing of other farnesylated proteins is related to toxicity, it is unlikely attributable to inhibition of Ras farnesylation alone.

**Toxicity Is Attributable to BMS-214662-induced Apoptosis in HCT-116 Human Colon Tumor Cells.** In general, BMS-214662-induced toxicity was observed in cells exposed for a duration  $>24$  h. To determine whether the toxicity was a result of apoptosis induction, HCT-116 human colon cells were exposed to the drug for the first 2 h, or 48 h of a 48-h incubation period, and apoptosis was determined by nucleosomal DNA ELISA assay. BMS-214662 caused an increase in nucleosomal DNA in the cytoplasm of cells without an increase in the medium (a marker for apoptosis). Although short drug exposure did lead to apoptosis, it required low micromolar concentrations (Fig. 3A). Drug exposure for 48 h resulted in apoptosis with submicromolar concentrations. These results suggest that drug exposures as short as 2 h prime HCT-116 cells to undergo apoptosis in 48 h.

BMS-214662 also induced apoptosis in H-Ras-transformed Rat1 CVLS cells, albeit at  $>10$ -fold higher concentrations, and required continuous 48-h exposure compared with the 2-h exposure for HCT-116 human colon tumor cells. Short drug exposures such as 2 h did not prime Rat1 CVLS cells to undergo apoptosis in 48 h. However, continuous 48-h exposures and high concentrations (1.6  $\mu\text{M}$ ) induced an increase in nucleosomal DNA in the cytoplasm of cells (Fig. 3B).

We next determined the time kinetics of apoptosis. HCT-116 cells were exposed to BMS-214662 for various periods of time, and apoptosis was immediately measured by the nucleosomal DNA ELISA assay. No detectable apoptosis, irrespective of the high drug concentration, occurred in the first 6 h (data not shown). Apoptosis was readily observed at 24 h with as little as 0.37  $\mu\text{M}$  BMS-214662. The minimal concentrations required for apoptosis did not differ appreciably for 24 and 48 h, suggesting a requirement for a certain threshold drug concentration. These results also suggest that the molecular events unleashed by BMS-214662 require a 24-h period to manifest in the form of apoptosis.

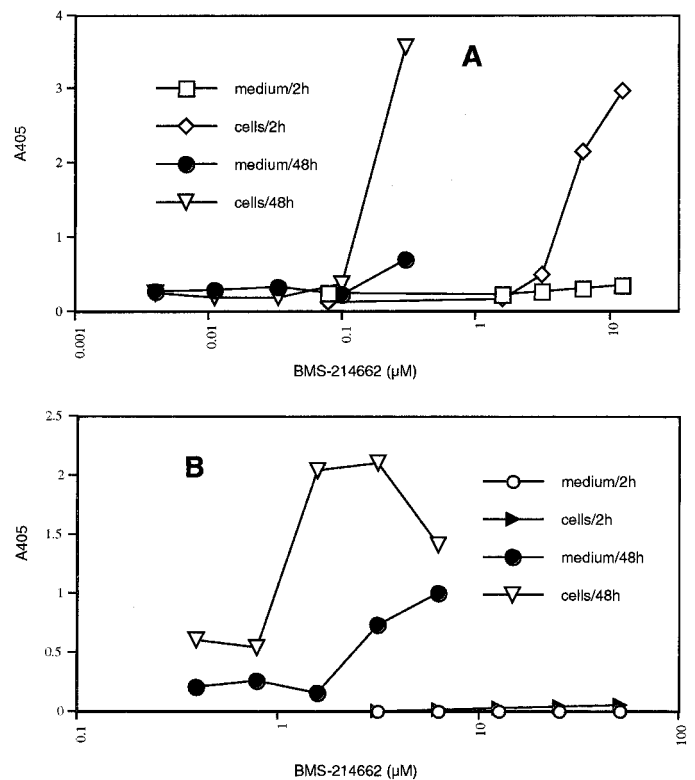


Fig. 3. A, kinetics of apoptosis induction in HCT-116 cells as measured by the increase of nucleosomal DNA in cell cytoplasm. B, kinetics of apoptosis induction in H-Ras-transformed Rat1 CVLS cells as measured by the increase of nucleosomal DNA in cell cytoplasm.

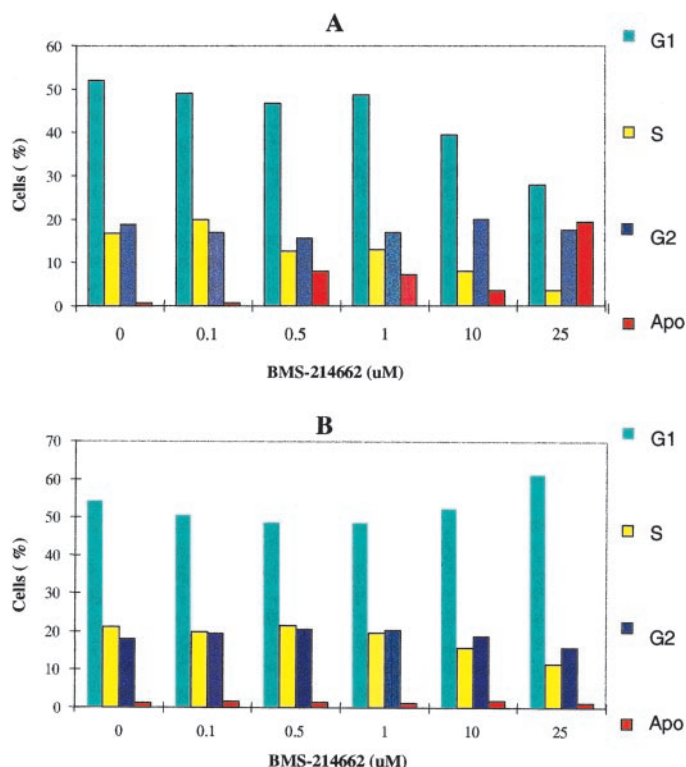


Fig. 4. A, effect of BMS-214662 on the cell cycle distribution and induction of apoptosis in HCT-116 cells. B, effect of BMS-214662 on the cell cycle distribution and induction of apoptosis in murine M109 lung tumor cells.

**Cell Cycle Analysis.** The effect of BMS-214662 on the cell cycle distribution and induction of apoptosis in HCT-116 cells was analyzed by flow cytometry. HCT-116 cells were exposed to compounds for 24 h and processed for cell cycle analysis with propidium iodide, and AI was determined by the TUNEL assay. BMS-214662-induced apoptosis was detectable at 0.5  $\mu\text{M}$ , with a majority of the apoptotic cells coming from the G<sub>1</sub> and S-phase cells (Fig. 4A). The number of apoptotic cells increased to 20% of the population at 25  $\mu\text{M}$ . A similar experiment performed with murine M109 lung tumor cells showed no increase in apoptotic cells at 25  $\mu\text{M}$  BMS-214662 (Fig. 4B).

The kinetics of apoptosis induction was also determined using flow cytometry and the TUNEL assay in HCT-116 cells. Cells were exposed to low concentrations (100 and 500 nM) of the drug for 12, 24, 48, 72, or 96 h, and the apoptotic cell numbers were determined. No significant apoptosis was observed with 100 nM BMS-214662 when cells were exposed for up to 48 h. There was measurable but minimal apoptosis when the exposure was extended to 72 h. The induction of apoptosis with 500 nM BMS-214662 was clearly detectable in the first 24-h exposure period. Further drug exposure to 48 or 72 h increased the extent of apoptosis dramatically from 5 to >50%. Near complete apoptosis was observed when cells were exposed to 500 nM BMS-214662 for 96 h.

**Cytotoxicity against Tumor Cell Line Panel.** Consistent with its potent apoptotic activity, BMS-214662 demonstrated potent *in vitro* cytotoxicity against a cell line panel consisting of human tumors, as well as mouse tumor and fibroblast cells and bovine normal endothelial cells. The data shown in Fig. 5 are expressed as IC<sub>50</sub>s for each cell line in a bar graph. The mean IC<sub>50</sub> was 0.20  $\mu\text{M}$ . The individual IC<sub>50</sub>s and the mean bar graph pattern illustrate that BMS-214662 has robust cell selectivity against a wide variety of tumor cell types. There was a >32-fold difference between the most sensitive and most resistant cell lines.

Particularly sensitive to BMS-214662 were human tumor lines OVCAR-3 ovarian, HCT-116 colon, A431 squamous, and HL60 leukemia. Conversely, both mouse cell lines, M109 lung carcinoma and MLF fibroblast, were relatively resistant to BMS-214662. Other cell lines were also relatively resistant to BMS-214662, including primary ABAE normal bovine endothelial cells and two human lung carcinoma cell lines. The sensitive cell lines A431 and OVCAR-3 did not have *ras* mutations, and a less sensitive cell line, LX-1, did have a mutated *ras*. Thus, *in vitro*, there appeared to be a lack of correlation between cytotoxicity to BMS-214662 and mutation status of *ras*.

HCT-116/VM46 and MIP colon cells both overexpress P-glycoprotein, a drug efflux pump, and are resistant to a number of lipophilic anticancer agents, such as paclitaxel, etoposide, and doxorubicin. The HCT-116/VM46 cells were 4-fold resistant to BMS-214662 relative to the parental HCT-116 cells, and MIP cells were 2-fold resistant relative to the mean IC<sub>50</sub> for all cell lines in the panel. These results suggest that BMS-214662 may be a weak substrate for P-glycoprotein.

### In Vivo Activity

**BMS-214662 versus HCT-116 Human Colon Carcinoma.** The initial discovery of antitumor activity associated with BMS-214662 was made after its oral administration, once qd for 10 days ( $\times 10$ ), Monday through Friday only, to mice bearing s.c. HCT-116 human colon tumors that ranged in size from 80 to 136 mg. Optimal treatment with the highest dose evaluated, 600 mg/kg/administration, which showed no evidence of being an MTD, cured eight of eight mice. Even the next lower dose tested, 300 mg/kg/administration, cured four of eight mice. A summary of this and other optimal antitumor effects is shown in Table 3.

In a subsequent experiment, treatment by the i.p. route using an intermittent injection schedule (400 mg/kg/injection, q4d $\times 4$ ), initiated on day 13 after tumor implant when tumors ranged in size from 138 to 319 mg, yielded six of seven cured mice.

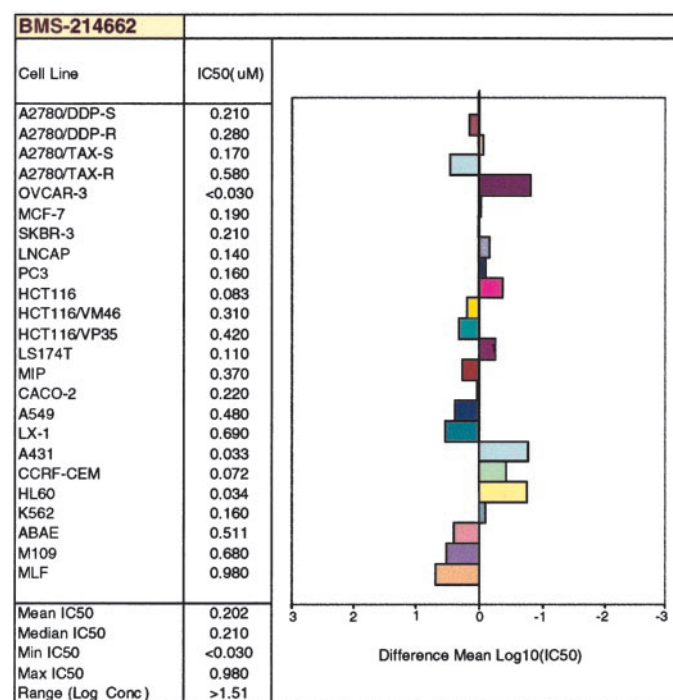


Fig. 5. *In vitro* cytotoxicity of BMS-214662 against a panel of tumor and normal cell lines. IC<sub>50</sub>s (expressed in micromolar) were determined after 72 h drug exposure using a tetrazolium dye conversion assay.

Table 3 Summary of optimal antitumor effects of BMS-214662

Tumor and route	Treatment schedule	Optimal dose (mg/kg/administration)	Cures/Total (or LCK)
<b>Human</b>			
HCT-116			
p.o.	qd × 10 (Monday–Friday)	600	8/8
i.p.	q4d × 4	400	6/7
Calu-1			
p.o.	qd × 14 (Monday–Friday)	800	4/8
HT-29			
i.p.	q4d × 4	450 <sup>a</sup>	6/8
EJ-1			
p.o.	qd × 14 (Monday–Friday)	600	8/8
i.p.	q4d × 4	300 <sup>a</sup>	5/8
i.v.	q3d × 5	175	6/7
HCT-116/VM46 <sup>b</sup>			
p.o.	qd × 10 (Monday–Friday)	600	3/7 (2.0)
MiaPaCa-2			
p.o.	qd × 10 (Monday–Friday)	600	4/7
N-87			
p.o.	2qd × 14 (Monday–Friday)	300	0/7 (0.9)
<b>Murine</b>			
LL			
i.p.	q2d × 5	400	(0)
M5076			
i.p.	q4d × 3	300 <sup>a</sup>	(0)
i.v.	q2d × 5	200	(0)

<sup>a</sup> Maximum tolerated dose probably reached.

<sup>b</sup> A cell line with a MDR phenotype.

**BMS-214662 versus Calu-1 Human Lung Carcinoma.** Additional antitumor testing with p.o.-administered BMS-214662 was carried out using the human lung carcinoma, Calu-1. The highest dose administered was escalated to 800 mg/kg/administration for 14 days (Monday–Friday), against tumors staged to a large average weight of about 250 mg (day 21 after tumor implant). At this maximum dose, BMS-214662 cured four of eight mice. The next lower dose, 500 mg/kg/administration, was effective (3.2 LCK) but not curative, and the next lower dose, 300 mg/kg/administration, was minimally active (1.2 LCK). This dose-response is illustrated in Fig. 6.

**BMS-214662 versus HT-29 Human Colon Carcinoma.** The HT-29 colon carcinoma (which has no *ras* mutation) was staged to 160–270 mg at the time of treatment initiation. BMS-214662 was administered i.p., using a q4d×4 treatment schedule. At the highest dose tested, 450 mg/kg/administration, which resulted in one mouse dying and therefore is considered the MTD, six of eight mice were cured (Fig. 7). The next lower dose, 300 mg/kg/administration, cured three of eight mice, and the lowest dose tested, 200 mg/kg/administration, was also effective (1.5 LCK).

**BMS-214662 versus EJ-1 Human Bladder Carcinoma.** The EJ-1 bladder carcinoma was staged to 50–100 mg at the time of treatment initiation. Both i.p. and p.o. routes of administration were compared. The highest p.o. dose of BMS-214662 evaluated, 600 mg/kg/administration, qd×14 (Monday–Friday), cured all eight mice treated; the next lower dose used, 300 mg/kg/administration, cured four of six mice. In comparison, the optimal effect obtained after i.p. injection of BMS-214662 was five of eight mice cured using an intermittent (300 mg/kg/administration; q4d×4) treatment schedule. This dose level was the MTD (the next higher dose was excessively toxic).

An additional EJ-1 experiment was used to characterize the i.v. antitumor activity of BMS-214662. The compound was formulated in 5% Tween 80 in water for i.v. administration. The sizes of the tumors at initiation of therapy were also larger (160–343 mg) than those used in the initial EJ-1 experiment. At the highest dose tested, 175 mg/kg/administration, six of seven mice were cured. The next lower dose tested, 125 mg/kg/administration, cured five of eight mice.

**BMS-214662 versus HCT-116/VM46 Human Colon Carcinoma.** An experiment was conducted in mice bearing HCT-116/VM46 to determine the efficacy of BMS-214662 against MDR tumors. The

optimal effect produced after p.o. administration of 600 mg/kg/administration, qd×10 (Monday–Friday), of BMS-214662 was 2.0 LCK accompanied by three of seven cures.

**BMS-214662 versus MiaPaCa-2 Human Pancreatic Carcinoma.** MiaPaCa-2 was staged to 104–188 mg at the time of treatment initiation. BMS-214662 was given p.o., qd×10 (Monday–Friday). At the highest dose evaluated, 600 mg/kg/administration, the compound was active, curing four of seven mice.

**BMS-214662 versus N-87 Human Gastric Carcinoma.** Mice bearing N-87 tumors were treated twice daily for 14 days, p.o., with BMS-214662 beginning on day 23 after tumor implant. At the highest dose tested, 300 mg/kg/administration, 0.9 LCK was produced with no cures.

**BMS-214662 versus Murine Tumors.** Two murine tumor models, LL and M5076 sarcoma, were also used to evaluate the therapeutic potential of BMS-214662. Against unstaged LL, i.p. treatment with BMS-214662, q2d×5, failed to demonstrate any activity (0 LCK) at doses as great as 400 mg/kg/administration (*i.e.*, well within the active range of doses as seen in the human tumor models). Against unstaged M5076, BMS-214662 was evaluated in two different vehicles, 5% Tween 80 and 10% ethanol (both in water diluents). The compound in 5% Tween 80 was administered i.v. on a q2d×5 schedule at doses as great as 200 mg/kg/administration. BMS-214662 in 10% ethanol was administered i.p., q4d×3, and reached the MTD at 300 mg/kg/administration. BMS-214662 was inactive (0 LCK) versus M5076 by both routes of administration.

**Schedule Dependency/Optimization.** The antitumor activity of BMS-214662 was found to be schedule independent but was cumulatively dose dependent. BMS-214662 was evaluated i.p. and p.o. against staged Calu-1 using different treatment schedules of identical duration in an attempt to discern an optimal treatment schedule or schedule dependency. All treatments began 20 days after tumor implant. Selected data from that experiment are summarized in Table 4.

When using i.p. injections involving qd treatment, twice a day treatment, or an intermittent treatment schedule of every third day, we observed similar therapeutic outcomes when cumulative dose exposures were compared. A cumulative dose of 1600–2000 mg/kg

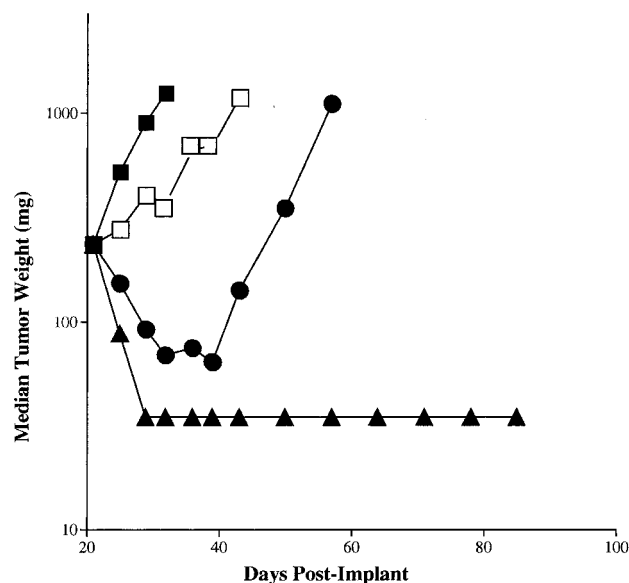


Fig. 6. Oral dose-response of BMS-214662. The compound was administered qd×14 (Monday–Friday only), p.o., versus advanced staged Calu-1 human lung carcinoma: ■, Control; ▲, BMS-214662 at 800 mg/kg/administration; ●, 500 mg/kg/administration; 127, 300 mg/kg/administration. Fifty % of the mice were cured at the 800 mg/kg/administration level.

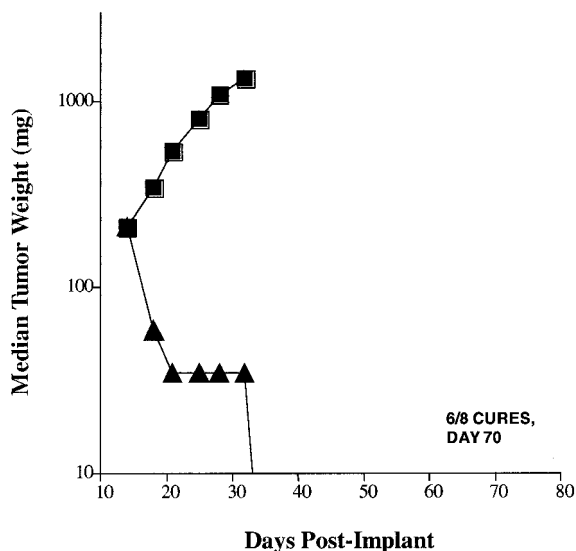


Fig. 7. Activity of BMS-214662 versus advanced staged HT-29 human colon carcinoma: ■, Control; ▲, BMS-214662 at 450 mg/kg/injection, i.p., administered q4d $\times$ 4 beginning day 12 postimplant.

yielded 1.4–1.6 LCK on the three schedules. A lower cumulative dose of 1200–1300 mg/kg produced an identical 0.9 LCK on all three schedules. For the two p.o. schedules evaluated, every day and every third day, cumulative doses of 3200–5000 mg/kg produced 1.5 LCK, indicating the need for roughly a 2-fold dose escalation of administered compound p.o. relative to i.p. to achieve comparable levels of activity. The best result observed in the experiment was associated with a p.o.-administered cumulative dose of 8000 mg/kg of BMS-214662, five of eight cures.

**Direct Cytotoxicity against Tumor Cells *in Vivo*.** Nude mice bearing the human carcinomas HCT-116 or EJ-1 were treated with BMS-214662 by i.v. infusion at various doses. At the end of treatment, tumors were excised, and tumor cell kill was determined by an *in vitro* colony formation assay. As shown in Fig. 8, BMS-214662 was significantly cytotoxic to both HCT-116 and EJ-1 tumor cells; the doses of BMS-214662 required to kill 90% of clonogenic tumor cells were approximately 75 and 100 mg/kg for HCT-116 and EJ-1 tumors, respectively.

**Apoptosis in Tumors.** Tumors from BMS-214662-treated mice had increased numbers of apoptotic cells as compared with the nontreated control mice (Fig. 9). Mean AIs from each group are presented in Table 5. The AIs in HCT-116 tumors were increased 4–10-fold in BMS-214662-treated mice as compared with nontreated controls. Highest AIs were observed in tumors from mice treated at 300 mg/kg or higher. These results, based on a limited sample size, indicate that tumor cell apoptosis is induced after BMS-214662 administration.

**Inhibition of FT and Ras Processing *in Vivo*.** To establish that BMS-214662 inhibited FT activity and blocked Ras processing in tumors of the treated mice, we performed FT assays and Ras Western blot assays. Extracts from control tumors and BMS-214662-treated tumors (6 and 24 h) were analyzed. The FT activity, as assayed using either H-Ras or K-Ras as the substrate, was inhibited by 95% in the tumor sample removed from mice 6 h after 300 mg/kg dose and remained inhibited by 85% in sample removed 24 h after dosing (Fig. 10) When the status of H-Ras processing the same tumor samples was analyzed, there was partial depletion of Ras in the particulate fraction and rapid accumulation of unprocessed Ras in the soluble fraction in tumors treated for 6 h; the depletion of Ras in the particulate fraction was near complete by 24 h (Fig. 10). These results establish the

pharmacological inhibition of FT and the resultant block in H-Ras processing in tumor xenografts treated with BMS-214662.

## DISCUSSION

BMS-214662 is a potent inhibitor of FT and is >1000-fold selective for FT over GGTI. We demonstrated previously that earlier lead compounds from these chemical series are competitive inhibitors with respect to the Ras protein substrate (49). BMS-214662 is also a competitive FTI with a  $K_i$  of 0.93 nM (H-Ras substrate). Consistent with its competitive nature and similar to other competitive FTIs (59), BMS-214662 exhibited 5-fold less potency when K-Ras was used as the substrate.

Our studies on the effect of BMS-214662 on morphological reversion with various cell lines imply H-Ras as the specific target. However, studies by others (32, 60) suggest that the morphological reversion of transformed cells caused by FTIs such as B581 and L-739,749 was independent of Ras function and was proposed to involve interference with RhoB activity. The FTIs used in these studies belong to distinct chemical classes but are potent and seemingly selective FTIs. Thus, although the basis for the differences between our results and those of others (32, 60) is not clear at present, these differences suggest that not all FTIs (belonging to different chemical classes) produce the same effects in cells. Despite its controversial nature (whether Ras or other protein involvement), our experience has been that the morphological reversion assay is a good measure of FT inhibition in cells and has been widely used for determining the whole cell activity of FTIs.

BMS-214662 inhibited the anchorage-independent growth of H-Ras- and K-Ras-transformed rodent fibroblasts but not MEK2-trans-

Table 4. Schedule dependency/optimization of BMS-214662 versus Staged Sc Calu-1 Human Lung Carcinoma

Treatment (per injection)	Route	Cumulative dose (mg/kg)	LCK (cures/total)
2qd $\times$ 10;20	i.p.	2000	1.6
		1300	0.9
qd $\times$ 10;20	i.p.	2000	1.4
		1300	0.9
q3d $\times$ 4; 20	i.p.	1600	1.5
		1200	0.9
qd $\times$ 10;20	p.o.	8000	(5/8)
		5000	1.5
q3d $\times$ 4; 20	p.o.	3200	1.5
		2000	1.0

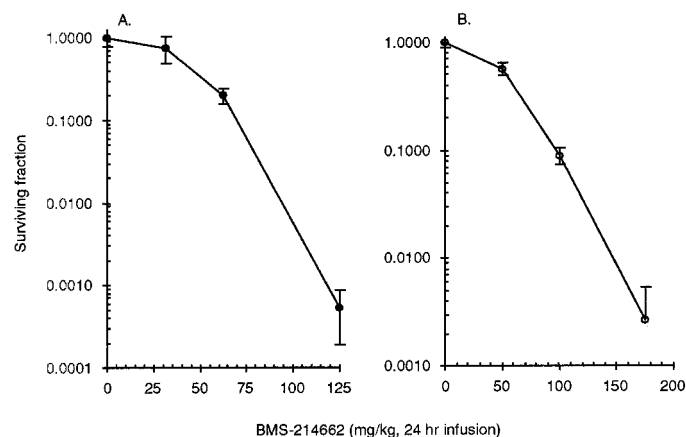


Fig. 8. Tumor clonogenic cell survival after 24-hr infusion of BMS-214662 as determined by the tumor excision assay. A, HCT-116 human colon carcinoma. B, EJ-1 human bladder carcinoma. Data are means; bars, 1 SD.

Fig. 9. Photomicrographs of a HCT-116 xenotransplanted tumor from a control (A) and 400 mg/kg p.o. BMS-214662 treated mouse at 24 h postdose (B). A mitotic figure and a low number of apoptotic cells are present in the nontreated control tumor. In contrast, many apoptotic cells are present in the BMS-214662-treated tumor. H&E stain,  $\times 400$ .

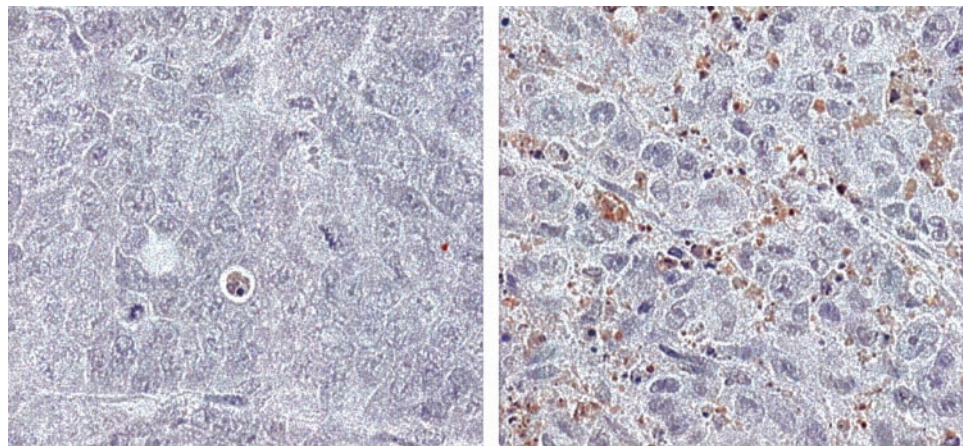


Table 5 Mean AIs in HCT-116 tumors 24 h after BMS-214662 administration

BMS-214662 (mg/kg)	n	Route	Mean AI (%)
0 (control tumor)	4		0.9
250	3	i.v.	3.7
300	3	i.p.	8.5
400	2	p.o.	9.0
400 (day 1)	2	p.o.	
400 (day 2)		i.p.	11.4

formed rodent cells. H-Ras-transformed cells are 10-fold more sensitive than K-Ras-transformed cells ( $IC_{50}$ , 0.025 versus 0.3  $\mu M$ ). The low sensitivity of K-Ras cells to BMS-214662 is consistent with an order of magnitude higher affinity of FT for K-Ras compared with the H-Ras proteins (59) and K-Ras geranylgeranylation in FTI-treated cells (37, 38). MEK2-transformed cells are not dependent on Ras function for SAG and are not significantly affected by BMS-214662. Thus, the effects of BMS-214662, particularly at low concentrations, in rodent cell models is consistent with Ras as the specific target.

BMS-214662 inhibited the SAG of human tumor cells, which usually contain multiple genetic aberrations, such as mutant Ras, mutant p53, up-regulated protein tyrosine kinase receptors, cell cycle alterations, and deregulated Myc expression. In addition, BMS-214662 targeted human tumor cells with or without Ras mutation and independent of K-Ras or H-Ras mutation. Similar conclusions were drawn by others using FTIs B581 and L-744,832 (23, 39). Overall, these results raise questions about Ras being the target for FTIs, and there is additional evidence that disconnects Ras, such as lack of correlation of Ras mutation with cytotoxic activity (see later).

BMS-214662 is one of the most potent of our tetrahydrobenzodiazepine FTIs in inducing apoptosis in HCT-116 human colon tumor cells. As brief an exposure as 2 h to 3  $\mu M$  BMS-214662 primes HCT-116 cells to eventually undergo apoptosis within 48 h, and longer exposures require relatively lower concentrations. Continuous exposure for 24–48 h resulted in apoptosis at 0.1–0.3  $\mu M$  BMS-214662, concentrations that are easily attainable in animals without undue toxicity. Although the observation that FTIs or agents that block isoprenylation of proteins by indirect mechanisms induce apoptosis in Ras-transformed rodent fibroblasts and in human tumor cells has been reported widely by others (31, 34, 61–67), apoptosis was observed either in specialized conditions (low serum or cell adhesion prevention) or with high micromolar concentrations. In contrast, BMS-214662 induced apoptosis at submicromolar concentrations in regular tissue culture medium with 10% serum. It is not clear at present whether and how BMS-214662-induced apoptosis differs from apoptosis reported for other FTIs. In our experience,

induction of apoptosis as reported here appears to be specific to the potent tetrahydrobenzodiazepine FTIs because other classes of inhibitors (phosphonate bisubstrate, thiol tetrapeptide, imidazolyl tetrapeptide, thioproline tetrapeptide, thiol piperazine, thioproline piperazine, thiol aminobenzoate, thiol dipeptide, thioproline dipeptide, and GGTI-specific tetrapeptide) did not induce significant apoptosis or caused only mild apoptosis/necrosis at very high concentrations (50–200  $\mu M$ ). Most of these compounds are roughly equipotent to the tetrahydrobenzodiazepine inhibitors in FT or cell reversion assays.

The high apoptotic potency of BMS-214662 prompted us to analyze the cytotoxic activity against a large panel of cell lines using the MTS assay. BMS-214662 is a potent cytotoxic agent *in vitro* against a wide variety of human tumor cell lines, including colon, breast, ovarian, prostate, and squamous cell carcinomas. Two mouse cell lines in the panel, a fibroblast and a carcinoma, were both relatively resistant to BMS-214662 when compared with most of the human carcinoma and human fibroblast cell lines. Although the murine sample size was limited, the possibility of a species difference in sensitivity remains possible.

Among the more sensitive cell lines ( $IC_{50}$  less than the mean; Fig. 5) were those lacking *ras* mutations (A431 and OVCAR-3) and with *ras* mutations (HCT-116, LS174T, and CCRF-CEM). Less sensitive cell lines that contained a mutated *ras* include LX-1, MIP, A549, and M109. This lack of correlation between Ras mutation status and sensitivity has been widely reported for a variety of FTIs (39–41, 68), and it has been hypothesized that the antitumor effects of FTIs involve inhibition of farnesylation of proteins other than Ras (15, 27, 42, 43). Although no single candidate protein has emerged as the true FTI target to date, interesting candidates include RhoB, RhoE, PRL-1 tyrosine phosphatases, centromere-associated CENP-E/F, nuclear lamins, and IP3 phosphatase (15, 42). The “FTI-Rho hypothesis” put forward by the Prendergast group has been supported by compelling evidence for FTI altering Rho-dependent cell adhesion, survival, and apoptosis signals (27–33, 69). However, data depicting RhoB as a tumor suppressor (70) and the apparent lack of correlation between

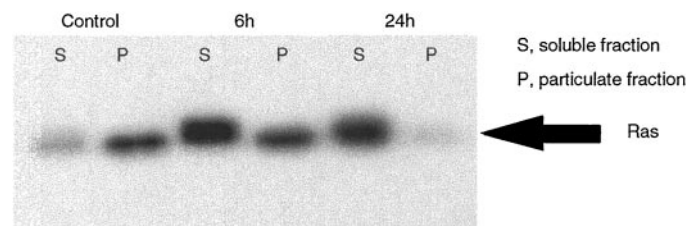


Fig. 10. Inhibition of H-Ras processing in HCT-116 tumors of mice treated with BMS-214662.

RhoB expression and FTI sensitivity in tumor cell lines (42) imply that the true target(s) of FTI remains to be identified. We also observed minimal resistance of MDR-containing cell lines toward BMS-214662, suggesting that our FTI, at best, may be a weak MDR substrate. One other FTI, SCH 66336, was reported recently to be a potent inhibitor of the MDR1 pump (71).

BMS-214662 was found to possess broad spectrum antitumor activity in human tumor xenografts of diverse histological sources. Curative activity against well-established tumors was demonstrated parenterally and *p.o.*, regardless of the presence or absence of *ras* mutations in the responding tumor lines. Our results are consistent with several published reports on FTI antitumor activity being independent of activated *ras* oncogene (21, 23, 40, 41, 68, 72). BMS-214662 sharply differs from other FTIs in terms of its potent tumor regression and curative potential. Other FTIs such as SCH66336, L-744,832, R115777, BIM-46228, FTI-277, B-956, and FTI-2153 primarily act as cytostatic drugs and produce noncurative regressions in transgenic tumor models or selected human tumor xenografts (22, 23, 40, 68, 72–76). BMS-214662 also retained good activity when a MDR tumor subline was evaluated for responsiveness and compared historically to the responses obtained with the parental line.

Despite the dramatic effects observed against human tumors, no activity was produced by BMS-214662 against two murine tumor models. We have also tested other FTIs, with structures similar to BMS-214662, against a murine tumor (Madison 109 lung carcinoma) with a known *Ras* mutation and failed to observe any antitumor effects.<sup>3</sup> It is our experience that the complete absence of activity *versus* commonly used murine tumor models is quite atypical of compounds possessing marked activity against so many different staged human tumors.

The resistance is not completely attributable to inhibition of processing of FT substrates such as *Ras* in M109 cells. BMS-214662 produces near complete inhibition of *Ras* processing in M109 cells treated with 500 nM for 48 h (data not shown) in comparison to the same occurring in sensitive HCT-116 cells treated with 100 nM for 24 h (Fig. 2B). BMS-214662 exhibited equipotency (H-*Ras* as the substrate) to the farnesyltransferase enzyme isolated from M109 cells as well as other sensitive cells (IC<sub>50</sub>, 2–3 nM). When K-*Ras* was used as the substrate, the enzyme from M109 and MLF cells (both resistant and mouse cells) showed significantly less potency compared with the enzyme from sensitive cells (IC<sub>50</sub>, 70 nM *versus* 5–20 nM). However, the enzyme from sensitive PC-3 cells also showed reduced K-*Ras* potency (IC<sub>50</sub>, 120 nM). We also compared the FT activity levels in the entire cell panel presented here and found no correlation between enzyme levels and sensitivity, despite the wide range of FT levels across the panel (varied from 2 to 160 fmol/μg protein). Thus, although we did find some differences such as inhibition of FT substrates requiring longer exposure and higher concentrations as well as FT being relatively insensitive with K-*Ras* as the substrate from M109 cells, it is not clear whether these characteristics are the basis for resistance, particularly given that the doses used in mice produce high micromolar concentrations lasting for 6–12 h.

Our *in vitro* cytotoxicity results with two murine cell lines are consistent with the relative *in vivo* antitumor activities (Fig. 5). However, it is surprising that HCT-116/VM46 human tumor responded well to BMS-214662 treatment (Table 3), although its *in vitro* cytotoxic potency is only 2-fold different from that of M109 cells (IC<sub>50</sub>, 0.31 *versus* 0.68 μM). Thus, although cytotoxicity is a major component of the human tumor regression activity reported here for BMS-214662, the effect of the compound on mouse tumors

may be predominantly cytostatic (see also later). Nonetheless, the apparent resistance of mouse tumors is perplexing and remains to be explored further.

BMS-214662 is a potent inhibitor of murine tumor cell growth *in vitro* (Table 2) and yet produced no significant growth inhibition *in vivo* (only 22% growth inhibition was observed toward the end of treatment period in LL). This apparent lack of activity may be a reflection of the intermittent dosing schedule used. Consistent with this interpretation, BMS-214662 and its close analogues did produce 40–60% inhibition of *Ras*-transformed Rat1 tumor growth in mice with once or twice daily dosing schedules (data not shown). Finally, we also reported that carcinogen-induced skin tumors in mice were susceptible to therapeutic intervention with BMS-214662 (77).

The tumor regression and cures described for several human tumor xenografts after a relatively short course of treatment with BMS-214662 raises the question as to what brought about such rapid reduction of tumor volume. Although enzyme inhibitors affecting FT may typically be considered as cytostatic agents or produce regressions in certain specified tumors, the outright destruction of tumors would be unexpected. Although tumor regressions lasting during the dosing period were reported with certain FTIs using *Ras* transgenic models (22, 72), rapid tumor regressions that last and result in cures have not been described with other FTIs published to date (22, 23, 40, 68, 72–76). From the *in vivo-in vitro* tumor excision assay, we determined that there was direct cytotoxicity inflicted on tumor cells *in vivo* after BMS-214662 treatment. Given that a single dose of 75 mg/kg given as *i.v.* infusion over 24 h produced 90% cell death in HCT-116 tumors (Fig. 8), it is not surprising that repeated and high-dose treatment (175–800 mg/kg) was highly curative.

With further regard to how BMS-214662 exerts its antitumor effects, we demonstrated inhibition of FT and H-*Ras* processing in the tumors of mice treated with BMS-214662. We also observed increased numbers of apoptotic cells in tumors of treated mice, and the extent of AIs in the tumors correlated well with the extent of tumor regression. We are currently exploring: (a) whether and how FT inhibition is related apoptotic potency; (b) the possibility that BMS-214662 targets a yet to be identified molecule “X” to induce apoptosis; and (c) the relation of FT and “X” to apoptosis and antitumor activity.

On the basis of its efficacy demonstrated *in vivo* against a variety of human tumors, BMS-214662 was selected for clinical development and is presently in Phase I clinical trials. Thus, BMS-214662 joins three other FTIs, R115777, SCH-66336, and L-778123 that are under various stages of development in the clinic (43).

## ACKNOWLEDGMENTS

We thank R. Ryseck for testing the tumor lines for *ras* mutations. We gratefully acknowledge the technical support provided by M. Arico, C. Burke, J. L. Clark, L. Cornell, K. Fager, K. Johnston, J. L. MacBeth, R. Peterson, S. Rex, R. Smykla, C. VanDeren, Mei-Li D. Wen, C. Ricca, J. Gullobrown, E. O'Rourke, H. Gray, and B. Penhallow. Finally, we appreciate the useful discussions held with G. Vite, T. Wong, and J. Hunt.

## REFERENCES

1. Barbacid, M. *ras* genes. *Annu. Rev. Biochem.*, 56: 779–827, 1987.
2. Boguski, M. S., and McCormick, F. Proteins regulating *Ras* and its relatives. *Nature (Lond.)*, 366: 643–654, 1993.
3. Medema, R. H., and J. L. Bos. The role of p21ras in receptor tyrosine kinase signaling. *Crit. Rev. Oncog.*, 4: 615–661, 1993.
4. Bourne, H. R., Sanders, D. A., and McCormick, F. The GTPase superfamily: a conserved switch for diverse cell functions. *Nature (Lond.)*, 348: 125–132, 1990.
5. Bourne, H. R., Sanders, D. A., and McCormick, F. The GTPase superfamily: conserved structure and molecular mechanism. *Nature (Lond.)*, 349: 117–127, 1991.

<sup>3</sup> Unpublished data.

6. McCormick, F. ras GTPase activating protein. Signal transmitter and signal terminator. *Cell*, *56*: 5–8, 1989.
7. McCormick, F. GTP binding and growth control. *Curr. Opin. Cell Biol.*, *2*: 181–184, 1990.
8. Bos, J. L. *ras* oncogenes in human cancer: a review. *Cancer Res.*, *49*: 4682–4689, 1989.
9. Hancock, J. F., Magee, A. I., Childs, J. E., and Marshall, C. J. All ras proteins are polyisoprenylated but only some are palmitoylated. *Cell*, *57*: 1167–1177, 1989.
10. Schafer, W. R., Trueblood, C. E., Yang, C. C., Mayer, M. P., Rosenberg, S., Poulter, C. D., Kim, S. H., and Rine, J. Enzymatic coupling of cholesterol intermediates to a mating pheromone precursor and to the ras protein. *Science (Wash. DC)*, *249*: 1133–1139, 1990.
11. Jackson, J. H., Cochrane, C. G., Bourne, J. R., Solski, P. A., Buss, J. E., and Der, C. J. Farnesol modification of Kirsten-ras exon 4B protein is essential for transformation. *Proc. Natl. Acad. Sci. USA*, *87*: 3042–3046, 1990.
12. Gibbs, J. B., Oliff, A., and Kohl, N. E. Farnesyltransferase inhibitors: Ras research yields a potential cancer therapeutic. *Cell*, *77*: 175–178, 1994.
13. Gibbs, J. B. Ras C-terminal processing enzymes—new drug targets? *Cell*, *65*: 1–4, 1991.
14. Tamanoi, F. Inhibitors of Ras farnesyltransferases. *Trends Biochem. Sci.*, *18*: 349–353, 1993.
15. Cox, A. D., and Der, C. J. Farnesyltransferase inhibitors and cancer treatment: targeting simply Ras? *Biochim. Biophys. Acta*, *1333*: F51–F71, 1997.
16. Gibbs, J. B., and Oliff, A. The potential of farnesyltransferase inhibitors as cancer chemotherapeutics. *Annu. Rev. Pharmacol. Toxicol.*, *37*: 143–166, 1997.
17. Lerner, E. C., Hamilton, A. D., and Sebt, S. M. Inhibition of Ras prenylation: a signaling target for novel anti-cancer drug design. *Anticancer Drug Des.*, *12*: 229–238, 1997.
18. Manne, V., Ricca, C. S., Brown, J. G., Tuomari, A. V., Yan, N., Patel, D., Schmidt, R., Lynch, M. J., Ciosek, C. P., Carboni, J. M., Robinson, S., Gordon, E. M., Barbacid, M., Seizinger, B. R., and Biller, S. A. Ras farnesylation as a target for novel antitumor agents: potent and selective farnesyl diphosphate analog inhibitors of farnesyltransferase. *Drug Dev. Res.*, *34*: 121–137, 1995.
19. James, G. L., Goldstein, J. L., Brown, M. S., Rawson, T. E., Somers, T. C., McDowell, R. S., Crowley, C. W., Lucas, B. K., Levinson, A. D., and Marsters, J., Jr. Benzodiazepine peptidomimetics: potent inhibitors of Ras farnesylation in animal cells [see comments]. *Science (Wash. DC)*, *260*: 1937–1942, 1993.
20. Kohl, N. E., Mosser, S. D., de Solms, S. J., Giuliani, E. A., Pompliano, D. L., Graham, S. L., Smith, R. L., Scolnick, E. M., Oliff, A., and Gibbs, J. B. Selective inhibition of ras-dependent transformation by a farnesyltransferase inhibitor [see comments]. *Science (Wash. DC)*, *260*: 1934–1937, 1993.
21. Kohl, N. E., Wilson, F. R., Mosser, S. D., Giuliani, E., de Solms, S. J., Conner, M. W., Anthony, N. J., Holtz, W. J., Gomez, R. P., Lee, T. J., and *et al.* Protein farnesyltransferase inhibitors block the growth of ras-dependent tumors in nude mice. *Proc. Natl. Acad. Sci. USA*, *91*: 9141–9145, 1994.
22. Kohl, N. E., Omer, C. A., Conner, M. W., Anthony, N. J., Davide, J. P., de Solms, S. J., Giuliani, E. A., Gomez, R. P., Graham, S. L., Hamilton, K., *et al.* Inhibition of farnesyltransferase induces regression of mammary and salivary carcinomas in ras transgenic mice [see comments]. *Nat. Med.*, *1*: 792–797, 1995.
23. Nagasu, T., Yoshimatsu, K., Rowell, C., Lewis, M. D., and Garcia, A. M. Inhibition of human tumor xenograft growth by treatment with the farnesyl transferase inhibitor B956. *Cancer Res.*, *55*: 5310–5314, 1995.
24. Bishop, W. R., Bond, R., Petrin, J., Wang, L., Patton, R., Doll, R., Njoroge, G., Catino, J., Schwartz, J., Windsor, W., *et al.* Novel tricyclic inhibitors of farnesyl protein transferase. Biochemical characterization and inhibition of Ras modification in transfected Cos cells. *J. Biol. Chem.*, *270*: 30611–30618, 1995.
25. Manne, V., Yan, N., Carboni, J. M., Tuomari, A. V., Ricca, C. S., Brown, J. G., Andahazy, M. L., Schmidt, R. J., Patel, D., Zahler, R., *et al.* Bisubstrate inhibitors of farnesyltransferase: a novel class of specific inhibitors of ras transformed cells. *Oncogene*, *10*: 1763–1779, 1995.
26. Gibbs, J. B., Graham, S. L., Hartman, G. D., Koblan, K. S., Kohl, N. E., Omer, C. A., and Oliff, A. Farnesyltransferase inhibitors versus Ras inhibitors. *Curr. Opin. Chem. Biol.*, *1*: 197–203, 1997.
27. Lebowitz, P. F., and Prendergast, G. C. Non-Ras targets of farnesyltransferase inhibitors: focus on Rho. *Oncogene*, *17*: 1439–1445, 1998.
28. Du, W., Liu, A., and Prendergast, G. C. Activation of the PI3'K-AKT pathway masks the proapoptotic effects of farnesyltransferase inhibitors. *Cancer Res.*, *59*: 4208–4212, 1999.
29. Du, W., Lebowitz, P. F., and Prendergast, G. C. Cell growth inhibition by farnesyltransferase inhibitors is mediated by gain of geranylgeranylated RhoB. *Mol. Cell Biol.*, *19*: 1831–1840, 1999.
30. Lebowitz, P. F., Davide, J. P., and Prendergast, G. C. Evidence that farnesyltransferase inhibitors suppress Ras transformation by interfering with Rho activity. *Mol. Cell Biol.*, *15*: 6613–6622, 1995.
31. Lebowitz, P. F., Sakamuro, D., and Prendergast, G. C. Farnesyl transferase inhibitors induce apoptosis of Ras-transformed cells denied substratum attachment. *Cancer Res.*, *57*: 708–713, 1997.
32. Prendergast, G. C., Davide, J. P., de Solms, S. J., Giuliani, E. A., Graham, S. L., Gibbs, J. B., Oliff, A., and Kohl, N. E. Farnesyltransferase inhibition causes morphological reversion of ras-transformed cells by a complex mechanism that involves regulation of the actin cytoskeleton. *Mol. Cell Biol.*, *14*: 4193–4202, 1994.
33. Prendergast, G. C., Khosravi-Far, R., Solski, P. A., Kurzawa, H., Lebowitz, P. F., and Der, C. J. Critical role of Rho in cell transformation by oncogenic *Ras*. *Oncogene*, *10*: 2289–2296, 1995.
34. Jiang, K., Coppola, D., Crespo, N. C., Nicosia, S. V., Hamilton, A. D., Sebt, S. M., and Cheng, J. Q. The phosphoinositide 3-OH kinase/AKT2 pathway as a critical target for farnesyltransferase inhibitor-induced apoptosis. *Mol. Cell Biol.*, *20*: 139–148, 2000.
35. Law, B. K., Norgaard, P., and Moses, H. L. Farnesyltransferase inhibitor induces rapid growth arrest and blocks p70s6k activation by multiple stimuli. *J. Biol. Chem.*, *275*: 10796–10801, 2000.
36. Ashar, H. A., James, L., Gray, K., Carr, D., Black, S., Armstrong, L., Bishop, R. W., and Kirschmeier, P. Farnesyl transferase inhibitors block the farnesylation of CENP-E and CENP-F and alter the association of CENP-E with the microtubules. *J. Biol. Chem.*, *275*: 30451–30457, 2000.
37. Whyte, D. B., Kirschmeier, P., Hockenberry, T. N., Nunez Oliva, I., James, L., Catino, J. J., Bishop, W. R., and Pai, J. K. K- and N-Ras are geranylgeranylated in cells treated with farnesyl protein transferase inhibitors. *J. Biol. Chem.*, *272*: 14459–14464, 1997.
38. Rowell, C. A., Kowalczyk, J. J., Lewis, M. D., and Garcia, A. M. Direct demonstration of geranylgeranylation and farnesylation of Ki-Ras *in vivo*. *J. Biol. Chem.*, *272*: 14093–14097, 1997.
39. Sepp-Lorenzino, L., Ma, Z., Rands, E., Kohl, N. E., Gibbs, J. B., Oliff, A., and Rosen, N. A peptidomimetic inhibitor of farnesyl:protein transferase blocks the anchorage-dependent and -independent growth of human tumor cell lines. *Cancer Res.*, *55*: 5302–5309, 1995.
40. Sun, J., Qian, Y., Hamilton, A. D., and Sebt, S. M. Ras CAAX peptidomimetic FTI 276 selectively blocks tumor growth in nude mice of a human lung carcinoma with K-Ras mutation and p53 deletion. *Cancer Res.*, *55*: 4243–4247, 1995.
41. Prevost, G. P., Pradines, A., Viostat, I., Brezak, M. C., Miquel, K., Lonchamps, M. O., Kasprzyk, P., Favre, G., Pignol, B., Le Breton, C., Dong, J., and Morgan, B. Inhibition of human tumor cell growth *in vitro* and *in vivo* by a specific inhibitor of human farnesyltransferase: BIM-46068. *Int. J. Cancer*, *83*: 283–287, 1999.
42. Cox, A. D., and Der, C. J. Farnesyltransferase inhibitors, anti-Ras or anticancer drugs. *In: J. S. Gutkind (ed.), Signaling Network and Cell Cycle Control: The Molecular Basis of Cancer and Other Diseases*. Totowa, NJ: Humana Press, Inc., 2000.
43. Adjei, A. A. Protein farnesyltransferase as a target for the development of anticancer drugs. *Drugs Future*, *25*: 1069–1079, 2000.
44. Sebt, S. M., and Hamilton, A. D. Farnesyltransferase and geranylgeranyltransferase I inhibitors in cancer therapy: important mechanistic and bench to bedside issues. *Exp. Opin. Investig. Drugs*, *9*: 2767–2782, 2000.
45. Prendergast, G. C. Farnesyltransferase inhibitors: antineoplastic mechanism and clinical prospects. *Curr. Opin. Cell Biol.*, *12*: 166–173, 2000.
46. Sebt, S. M., and Hamilton, A. D. Inhibition of Ras prenylation: a novel approach to cancer chemotherapy. *Pharmacol. Ther.*, *74*: 103–114, 1997.
47. Lobell, R. B., and Kohl, N. E. Pre-clinical development of farnesyltransferase inhibitors. *Cancer Metastasis Rev.*, *17*: 203–210, 1998.
48. Ashar, H., Armstrong, L., James, L., Carr, D. M., Gray, K., Taveras, A., Doll, R. J., Bishop, R. W., and Kirschmeier, P. T. Biological effects and mechanism of action of farnesyltransferase inhibitors. *Chem. Res. Toxicol.*, *13*: 949–952, 2000.
49. Hunt, J. T., Ding, C. Z., Batorsky, R., Bednarz, M., Bhide, R., Cho, Y., Chong, S., Chao, S., Gullo-Brown, J., Guo, P., Kim, S.-H., Lee, F. Y. F., Leftheris, K., Miller, A., Mitt, T., Patel, M., Penhallow, B. A., Ricca, C., Rose, W. C., Schmidt, R., Slusarchyk, W. A., Vite, G., and Manne, V. The discovery of (R)-7-cyano-2,3,4,5-tetrahydro-1-(1H-imidazol-4-ylmethyl)-3-(phenylmethyl)-4-(2-thienylsulfonyl)-1H-1,4-benzodiazepine (BMS-214662), a farnesyltransferase inhibitor with potent preclinical antitumor activity. *J. Med. Chem.*, *43*: 3587–3595, 2000.
50. Rapp, U. R., Goldsborough, M. D., Mark, G. E., Bonner, T. E., Reynolds, F. H., Jr., and Stephenson, J. R. Structure and biological activity of *v-raf*, a unique oncogene transduced by a retrovirus. *J. Virol.*, *45*: 914–924, 1983.
51. Stanton, V. P., Jr., Nichols, D. W., Laudano, A. P., and Cooper, J. M. Definition of the human raf amino-terminal regulatory region by deletion mutagenesis. *Mol. Cell Biol.*, *9*: 639–647, 1989.
52. Long, B. H., Wang, L., Lorico, A., Wang, R. R. C., Brattain, M. G., and Casazza, A. M. Mechanisms of resistance to etoposide and teniposide in acquired resistant human colon and lung carcinoma cell lines. *Cancer Res.*, *51*: 5275–5284, 1991.
53. Giannakakou, P., Sacket, D. L., Kang, Y.-K., Zhan, Z., Buters, J. T. M., Fojo, T., and Poruchynsky, M. S. Paclitaxel-resistant human ovarian cancer cells have mutant  $\beta$ -tubulins that exhibit impaired paclitaxel-driven polymerization. *J. Biol. Chem.*, *272*: 17118–17125, 1997.
54. Kerr, J. F. R., Wyllie, A. H., and Currie, A. R. Apoptosis. A basic biological phenomenon with wide-ranging implications in tissue kinetics. *Br. J. Cancer*, *26*: 239–257, 1972.
55. Wheeldon, E. B., Williams, S. M., Soames, A. R., James, N. H., and Roberts, R. A. Quantitation of apoptotic bodies in rat liver by *in situ* end labeling (ISEL): correlation with morphology. *Toxicol. Pathol.*, *23*: 410–416, 1995.
56. Goalstone, M., Leitner, J. W., and Draznin, B. GTP loading of farnesylated p21Ras by insulin at the plasma membrane. *Biochem. Biophys. Res. Commun.*, *239*: 42–45, 1997.
57. Ulsh, L. S., and Shih, T. Y. Metabolic turnover of human c-rasH p21 protein of EJ bladder carcinoma and its normal cellular and viral homologs. *Mol. Cell Biol.*, *4*: 1647–1652, 1984.
58. James, G., Goldstein, J. L., and Brown, M. S. Resistance of K-RasBV12 proteins to farnesyltransferase inhibitors in Rat1 cells. *Proc. Natl. Acad. Sci. USA*, *93*: 4454–4458, 1996.
59. James, G. L., Goldstein, J. L., and Brown, M. S. Polylysine and CVIM sequences of K-RasB dictate specificity of prenylation and confer resistance to benzodiazepine peptidomimetic *in vitro*. *J. Biol. Chem.*, *270*: 6221–6226, 1995.
60. Cox, A. D., Garcia, A. M., Westwick, J. K., Kowalczyk, J. J., Lewis, M. D., Brenner, D. A., and Der, C. J. The CAAX peptidomimetic compound B581 specifically blocks farnesylation, but not geranylgeranylation or myristylation, oncogenic Ras signaling and transformation. *J. Biol. Chem.*, *269*: 19203–19206, 1994.

61. Wang, W., and McCaulay, R. J. Apoptosis of medulloblastoma cells *in vitro* follows inhibition of farnesylation using manumycin A. *Int. J. Cancer*, *82*: 430–434, 1999.
62. Suzuki, N., Urano, J., and Tamanoi, F. Farnesyltransferase inhibitors induce cytochrome *c* release and caspase 3 activation preferentially in transformed cells. *Proc. Natl. Acad. Sci. USA*, *95*: 15356–15361, 1998.
63. Vitale, M., Di Matola, T., Rossi, G., Laezza, C., Fenzi, G., and Bifulco, M. Prenyltransferase inhibitors induce apoptosis in proliferating thyroid cells through a p53-independent CrmA-sensitive, and caspase-3-like protease-dependent mechanism. *Endocrinology*, *140*: 698–704, 1999.
64. Sepp Lorenzino, L., and Rosen, N. A farnesyl-protein transferase inhibitor induces p21 expression and G1 block in p53 wild type tumor cells. *J. Biol. Chem.*, *273*: 20243–20251, 1998.
65. Feldkamp, M. M., Lau, N., and Guha, A. Growth inhibition of astrocytoma cells by farnesyl transferase inhibitors is mediated by a combination of anti-proliferative, pro-apoptotic and anti-angiogenic effects. *Oncogene*, *18*: 7514–7526, 1999.
66. Song, S. Y., Meszoely, I. M., Coffey, R. J., Pietenpol, J. A., and Leach, S. D. K-Ras-independent effects of the farnesyl transferase inhibitor L-744,832 on cyclin B1/Cdc2 kinase activity, G2/M cell cycle progression and apoptosis in human pancreatic ductal adenocarcinoma cells. *Neoplasia*, *2*: 261–272, 2000.
67. Di Paolo, A., Danesi, R., Nardini, D., Bocci, G., Innocenti, F., Fogli, S., Barachini, S., Marchetti, A., Bevilacqua, G., and Del Tacca, M. Manumycin inhibits ras signal transduction pathway and induces apoptosis in COLO320-DM human colon tumour cells. *Br. J. Cancer*, *82*: 905–912, 2000.
68. End, D. W., Smets, G., Todd, A. V., Applegate, T. L., Fuery, C. J., Angibaud, P., Venet, M., Sanz, G., Poignet, H., Skrzat, S., Devine, A., Wouters, W., and Bowden, C. Characterization of the antitumor effects of the selective farnesyl protein transferase inhibitor R115777 *in vivo* and *in vitro*. *Cancer Res.*, *61*: 131–137, 2001.
69. Liu, A. X., Du, W., Liu, J. P., Jessell, T. M., and Prendergast, G. C. RhoB alteration is necessary for apoptotic and antineoplastic responses to farnesyltransferase inhibitors. *Mol. Cell. Biol.*, *20*: 6105–6113, 2000.
70. Chen, Z., Sun, J., Pradines, A., Favre, G., Adnane, J., and Sebt, S. M. Both farnesylated and geranylgeranylated RhoB inhibit malignant transformation and suppress human tumor growth in nude mice. *J. Biol. Chem.*, *275*: 17974–17978, 2000.
71. Johnson, W. W., Wang, E., Obrocea, M., Casciano, C., and Clement, R. The farnesyl protein transferase inhibitor SCH66336 is a potent inhibitor of MDR1 product P-glycoprotein. *Proc. Am. Assoc. Cancer Res.*, *42*: abstract 1409, 261, 2001.
72. Liu, M., Bryant, M. S., Chen, J., Lee, S., Yaremko, B., Lipari, P., Malkowski, M., Ferrari, E., Nielsen, L., Prioli, N., Dell, J., Sinha, D., Syed, J., Korfmacher, W. A., Nomeir, A. A., Lin, C. C., Wang, L., Taveras, A. G., Doll, R. J., Njoroge, F. G., Mallams, A. K., Remiszewski, S., Catino, J. J., Girijavallabhan, V. M., Bishop, W. R., *et al.* Antitumor activity of SCH 66336, an orally bioavailable tricyclic inhibitor of farnesyl protein transferase, in human tumor xenograft models and wap-ras transgenic mice. *Cancer Res.*, *58*: 4947–4956, 1998.
73. Norgaard, P., Law, B., Joseph, H., Page, D. L., Shyr, Y., Mays, D., Pietenpol, J. A., Kohl, N. E., Oliff, A., Coffey, R. J., Poulsen, H. S., and Moses, H. L. Treatment with farnesyl-protein transferase inhibitor induces regression of mammary tumors in transforming growth factor (TGF)  $\alpha$  and TGF  $\alpha$ /neu transgenic mice by inhibition of mitogenic activity and induction of apoptosis. *Clin. Cancer Res.*, *5*: 35–42, 1999.
74. Barrington, R. E., Subler, M. A., Rands, E., Omer, C. A., Miller, P. J., Hundley, J. E., Koester, S. K., Troyer, D. A., Bearss, D. J., Conner, M. W., Gibbs, J. B., Hamilton, K., Koblan, K. S., Mosser, S. D., O'Neill, T. J., Schaber, M. D., Senderak, E. T., Windle, J. J., Oliff, A., and Kohl, N. E. A farnesyltransferase inhibitor induces tumor regression in transgenic mice harboring multiple oncogenic mutations by mediating alterations in both cell cycle control and apoptosis. *Mol. Cell. Biol.*, *18*: 85–92, 1998.
75. Sun, J., Blaskovich, M. A., Knowles, D., Qian, Y., Ohkanda, J., Bailey, R. D., Hamilton, A. D., and Sebt, S. M. Antitumor efficacy of a novel class of non-thiol-containing peptidomimetic inhibitors of farnesyltransferase and geranylgeranyltransferase I: combination therapy with the cytotoxic agents cisplatin, Taxol, and gemcitabine. *Cancer Res.*, *59*: 4919–4926, 1999.
76. Prevost, G. P., Pradines, A., Brezak, M. C., Lonchamp, M. O., Viossat, I., Ader, I., Toulas, C., Kasprzyk, P., Gordon, T., Favre, G., and Morgan, B. Inhibition of human tumor cell growth *in vivo* by an orally bioavailable inhibitor of human farnesyltransferase BIM-46228. *Int. J. Cancer*, *91*: 718–722, 2001.
77. Bol, D. K., Dell, J., Ho, C. P., Swerdel, M., Ricca, C., and Manne, V. A comparison of the therapeutic and preventative efficacy of a novel Ras farnesyltransferase inhibitor in endogenous mouse carcinogenesis models. *Proc. Am. Assoc. Cancer Res.*, *41*: 220, 2000.